JCTC Journal of Chemical Theory and Computation

Article

pubs.acs.org/JCTC

Electrochemical Solvent Reorganization Energies in the Framework of the Polarizable Continuum Model

Soumya Ghosh,[‡] Samantha Horvath,[†,‡] Alexander V. Soudackov, and Sharon Hammes-Schiffer*

Department of Chemistry, University of Illinois at Urbana−Champaign, 600 South Mathews Avenue, Urbana, Illinois 61801, United States

Supporting Information

ABSTRACT: Electron transfer reactions at electrochemical interfaces play a critical role in a wide range of catalytic processes. A key parameter in the rate constant expressions for such processes is the reorganization energy, which reflects the energetic cost of the solute and solvent rearrangements upon electron transfer. In this paper, we present dielectric continuum methods for calculating the solvent reorganization energy for electrochemical processes. We develop a method for calculating the electrochemical solvent reorganization energies with molecular-shaped cavities within the framework of the polarizable continuum model (PCM). The electronic and inertial responses of the solvent are separated according to their respective time scales, and two limiting cases of the relation between the solute and solvent electrons are examined. The effects of the electrode are included with the integral equations formalism PCM (IEF-PCM), in which the molecule-solvent boundary is treated explicitly, but the effects of the electrode-solvent boundary are included through an external Green's function. This approach accounts for the effects of detailed molecular charge redistribution in a molecular-shaped cavity, as well as the electronic and inertial solvent responses and the effects of the electrode. The calculated total reorganization energies are in reasonable agreement with experimental measurements for a series of electrochemical systems. Inclusion of the effects of the electrode is found to be essential for obtaining even qualitatively accurate solvent reorganization energies. These approaches are applicable to a wide range of systems and can be extended to include other types of boundaries, such as a self-assembled monolayer or double layer separating the electrode and the molecule.

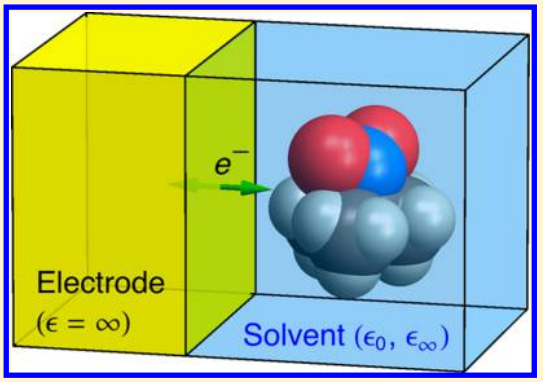

1. INTRODUCTION

Electron transfer reactions at electrochemical interfaces play an essential role in a wide range of catalytic processes.[1−7] The rate constants of electrochemical electron transfer (ET) reactions can be computed in the framework of Marcus theory or extensions of Marcus theory.[8−18] In such theories, a key parameter in the rate constant expression is the reorganization energy, which is a measure of the energetic cost of the solute and solvent reorganization in response to the charge transfer between the solute and the electrode. The reorganization energy is often separated into an inner-sphere (solute) and an outer-sphere (solvent) component, although this separation is not rigorous. The inner-sphere reorganization energy is associated with the rearrangement of the solute geometry, and the solvent reorganization energy is associated with the rearrangement of the solvent environment upon ET. In turn, the solvent response is divided into fast and slow time scale motions, where the fast time scale response is attributed mainly to the electronic degrees of freedom and the slow time scale response is attributed mainly to the translational and rotational solvent degrees of freedom.

A variety of computational approaches have been developed to calculate the inner-sphere and outer-sphere reorganization energies.[8,19−27] The inner-sphere reorganization energy can be calculated with an approach based on a harmonic normal mode approximation for the changes in bond lengths upon oxidation or reduction of the molecule[8,24,25] or with the "four-point method,"[19] which utilizes the energies of the reduced and oxidized states at the two respective equilibrium geometries. Both of these approaches are straightforward to implement. The solvent reorganization energy can be calculated with either a dielectric continuum representation of the solvent or a molecular representation of the solvent in conjunction with molecular dynamics simulations. Both approaches have been developed extensively for homogeneous ET reactions in solution[28−37] but have not been explored as much for electrochemical ET reactions.[38−42]

This paper focuses on the development of a dielectric continuum approach for the calculation of the electrochemical solvent reorganization energy. For homogeneous ET in solution, the simplest approach is to represent the donor and acceptor molecules as identical spheres separated by a specified distance in a dielectric continuum solvent. Within this model,

Received: January 21, 2014
Published: March 19, 2014

   dx.doi.org/10.1021/ct500051e | J. Chem. Theory Comput. 2014, 10, 2091−2102

the solution of the classical electrostatic equations yields the well-known Marcus expression for the solvent reorganization energy.[8] Moreover, the calculation of solvent reorganization energies for homogeneous ET has been extended to molecular-shaped cavities within the framework of the polarizable continuum model (PCM).[21,22,43] For electrochemical ET, the simplest approach is to represent the solute as a point charge within a sphere that is immersed in a dielectric continuum solvent and is located at a specified distance from the electrode surface. The analytical solution of the classical electrostatic equations for this model is also well known.[8,20,44] Herein, we extend this approach to the representation of the solute as a collection of point charges corresponding to the partial atomic charges of the molecule in a sphere located a specified distance from the electrode surface. In this case, the solution is numerical rather than analytical, but the results are found to be similar to those obtained with the simpler analytical expression.

The main advance in this paper is the development of a method for calculating the electrochemical solvent reorganization energies with molecular-shaped cavities within the framework of PCM. Our approach separates the fast and slow time scale responses of the solvent following the methodology developed earlier for homogeneous ET.[45−48] We explore two strategies for treating the fast solvent response, corresponding to two limiting cases of the relation between the time scales for the solvent and solute electrons. In the Born−Oppenheimer (BO) approach, the solvent electrons are assumed to move on a much faster time scale than the solute electrons, including the transferring electron. Thus, they contribute to the external potential for the solute electrons, analogous to the adiabatic potential energy surface for the nuclei in the standard Born−Oppenheimer separation between electrons and nuclei. In the alternative self-consistent (SC) approach, the solvent electrons are assumed to move on a much slower time scale than the solute electrons. Within the framework of dielectric continuum theory,[45,49,50] this limit corresponds to the self-consistent treatment of the delocalized charge density of the solute and the noninertial part of the solvent polarization describing the response of the solvent electrons. Our results indicate that these two approaches lead to very similar results for the reorganization energy.

To include the effects of the electrode, we utilize the integral equations formalism PCM (IEF-PCM), in which the molecule-solvent boundary is treated explicitly, but the effects of the electrode-solvent boundary are included through an external Green's function. This approach can be easily extended to include other types of boundaries, such as a self-assembled monolayer or double layer separating the electrode and the molecule. We test this approach on a series of systems for which experimental reorganization energies have been reported. Our results indicate that inclusion of the electrode response to ET is critical for obtaining even qualitatively accurate values of electrochemical solvent reorganization energies.

An outline of the paper is as follows. Section 2 presents the theoretical and computational methods. Section A describes the methods for calculating the inner-sphere reorganization energy as well as the analytical method for calculating the electrochemical solvent reorganization energy. Section B provides details on the separation of the electronic and inertial components of the solvent polarization, which are related to the fast and slow time scale responses, respectively, and section C presents the methodology for including the response of the electrode using the IEF-PCM formalism. Section D discusses the relation between the calculated quantities and the experimentally measured properties, including the choice of the distance of the molecule from the electrode surface. The computational details are provided in section E. Section 3 presents the results and a comparison between calculated and experimental reorganization energies. The concluding remarks and future directions are discussed in section 4.

2. THEORY AND COMPUTATIONAL METHODS

A. Inner-Sphere and Solvent Reorganization Energies.

Electron transfer between an electrode and a solute molecule in solution is accompanied by both structural rearrangement within the solute molecule and rearrangement of the surrounding solvent to accommodate the change in electronic density. The energy associated with the internal structural changes of the solute is referred to as the inner-sphere reorganization energy, denoted λ_i, and the energy associated with the rearrangement of the solvent at a fixed geometry of the solute is referred to as the outer-sphere or solvent reorganization energy, denoted λ_s. Typically, these two terms are assumed to be uncoupled and additive, although this separation is not rigorous.

The inner-sphere reorganization energy can be evaluated using several different approaches. In the harmonic approximation, the inner-sphere reorganization energy can be calculated using the force constants for the normal modes of the oxidized and reduced species and the shifts in the equilibrium values of the corresponding normal mode coordinates.[8,24,25] Alternatively, the inner-sphere reorganization energy can be obtained from standard quantum chemical calculations of the oxidized and reduced species in the gas phase:[19]

$$\lambda_i = \frac{1}{2}[\lambda_i^{(ox)} + \lambda_i^{(red)}] = \frac{1}{2}[E_{ox}(R_{eq}^{red}) - E_{ox}(R_{eq}^{ox}) + E_{red}(R_{eq}^{ox}) - E_{red}(R_{eq}^{red})] \quad (1)$$

In this expression, $\lambda_i^{(ox)}$ and $\lambda_i^{(red)}$ are the inner-sphere reorganization energies associated with the oxidized and reduced species, respectively, R_{eq}^{ox} and R_{eq}^{red} are the optimized equilibrium geometries of the oxidized and reduced species, respectively, and E_{ox} and E_{red} are the energies of the oxidized and reduced states, respectively, evaluated at the designated geometry.

The calculation of the solvent reorganization energy, however, is more involved. In the simplest case, the solute molecule can be represented as a point charge located at the center of a sphere, and the solvent is represented by a homogeneous dielectric continuum medium characterized by a dielectric constant ε. In this case, the change in the electrostatic potential, ϕ, corresponding to the change in the point charge, Δq, can be calculated using the following Poisson equation:[44]

$$\nabla^2\phi = -\frac{4\pi\Delta q\delta(\mathbf{r})}{\varepsilon} \quad (2)$$

If the point charge is placed at a distance d along the z-axis perpendicular to the surface of the electrode, which is assumed to have infinite dielectric constant, then the change in the electrostatic potential at a point with cylindrical coordinates (ρ, z, φ) with the origin at the point charge location (see Figure 1) can be expressed as[20,44]

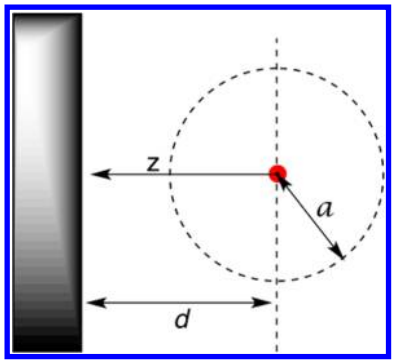

Figure 1. Schematic representation of the point-charge model for electrochemical electron transfer. The origin used for the cylindrical coordinates in the associated equations in the text is at the point charge (red circle), and the z-axis is defined as shown. The sphere has radius a, and the center of the sphere is a distance d from the electrode.

$$\phi(\rho, z) = \frac{\Delta q}{\varepsilon}\left[\frac{1}{(\rho^2 + z^2)^{1/2}} - \frac{1}{(\rho^2 + (2d - z)^2)^{1/2}}\right] \tag{3}$$

Assuming that the electrostatic potential does not vary significantly on the spherical surface, the conducting sphere approximation can be invoked. In this case, the average potential $\bar{\phi}$ is calculated on a hypothetical spherical surface with radius a surrounding the point charge, as shown in Figure 1. This averaging procedure is summarized in the Appendix, and the resulting average potential is given as

$$\bar{\phi} = \frac{\Delta q}{\varepsilon}\left(\frac{1}{a} - \frac{1}{2d}\right) \tag{4}$$

To compute the solvent reorganization energy using the above expression, the electronic and inertial components of the solvent polarization must be separated, as discussed in the next subsection. The expression for the solvent reorganization energy in terms of the average potentials $\bar{\phi}_0$ and $\bar{\phi}_\infty$ calculated with the static dielectric constant ε_0 and the optical dielectric constant ε_∞, respectively, is given as[20]

$$\lambda_s = \frac{1}{2}\Delta q(\bar{\phi}_\infty - \bar{\phi}_0) = \frac{(\Delta q)^2}{2}\left(\frac{1}{\varepsilon_\infty} - \frac{1}{\varepsilon_0}\right)\left(\frac{1}{a} - \frac{1}{2d}\right) \tag{5}$$

This reorganization energy is associated with the inertial component of the solvent polarization, as will be discussed further in the next subsection. In the limit of $d \to \infty$, this expression reduces to the expression for reorganization energy obtained from the Born solvation model.[51,52] We have extended this method to include a collection of atomic partial charges, as described in the Supporting Information.

B. Electronic Structure Methods for Calculating Solvent Reorganization Energies. The formulation and implementation of the polarizable continuum model (PCM) has been presented and discussed throughout the literature.[53−55] If nonelectrostatic effects are neglected, the equilibrium solvation free energy, ΔG_{eq}, is expressed in terms of the solute charge density, $\rho(\mathbf{r})$, and the solvent polarization potential, $\Phi(\mathbf{r})$, using the following standard relation of classical electrostatics:[44]

$$\Delta G_{eq} = \frac{1}{2}\int \Phi(\mathbf{r})\rho(\mathbf{r})\mathrm{d}^3\mathbf{r} \tag{6}$$

Here, we are neglecting the effects of the solvent on the solute charge density. In the discussions below, the dependence of the charge density and the solvent polarization potential on the spatial coordinate $\mathbf{r}$ is omitted for simplicity. In a nonequilibrium situation, such as a vertical excitation or solvent reorganization during ET, the total polarization must be separated into the electronic and inertial components.

B1. Separation of Electronic and Inertial Polarization. The total polarization can be expressed as the sum of the electronic and inertial components. The electronic component Φ_∞, which may also include contributions from other high-frequency motions, is characterized by the optical dielectric constant ε_∞. The inertial polarization, which is defined to be the difference between the total polarization and the electronic polarization, describes the slower degrees of freedom of the solvent.

The total solvent polarization potential Φ depends on the static dielectric constant ε_0. The inertial polarization potential Φ_{in} can be obtained from the difference between the total and electronic polarization potentials, $\Phi_{in} = \Phi - \Phi_\infty$. After splitting the total polarization into its components, the free energy of the solvated molecule can be expressed in a more general way as a functional of the inertial solvent polarization:[47]

$$G[\Phi_{in}] = -\frac{1}{2}\int \Phi_{in}\rho_{in}\mathrm{d}^3\mathbf{r} - \frac{1}{2}\int \Phi_\infty\rho_\infty\mathrm{d}^3\mathbf{r} + \int (\Phi_{in} + \Phi_\infty)\rho\mathrm{d}^3\mathbf{r} + G^0[\rho] \tag{7}$$

The first and second terms in eq 7 are the "self-energy" terms for the inertial and electronic components, respectively. The third term is the electrostatic interaction of the total solvent polarization potential Φ with the solute charge density ρ, and the last term is the gas phase free energy of the solute with a solvent polarized charge density, which is also referred to as the internal free energy of the solute.[47] In this notation, the densities ρ_{in} and ρ_∞ are in equilibrium with the polarization potentials Φ_{in} and Φ_∞, respectively, and ρ is in equilibrium with the total polarization potential, $\Phi = \Phi_{in} + \Phi_\infty$. For the case in which all polarization potentials, Φ, Φ_∞, and Φ_{in}, are in equilibrium with the same charge density, $\rho = \rho_\infty = \rho_{in}$, the first three terms of eq 7 reduce to eq 6.

In Marcus theory, electrochemical ET reactions can be described in terms of two electronic states corresponding to the oxidized and reduced states of the solute. Within linear response theory, the free energies of these states can be represented as quadratic functionals of the inertial component of the solvent polarization potential, which plays the role of the reaction coordinate for the ET reaction. In the case when the two electronic states are characterized by the fixed total charge densities, ρ^{ox} and ρ^{red}, the corresponding free energy functionals, $G_{ox}[\Phi_{in}]$ and $G_{red}[\Phi_{in}]$, describing both equilibrium and nonequilibrium free energies are given by

$$G_i[\Phi_{in}] = -\frac{1}{2}\int \Phi_{in}\rho_{in}\mathrm{d}^3\mathbf{r} - \frac{1}{2}\int \Phi_\infty^i\rho_\infty^i\mathrm{d}^3\mathbf{r} + \int (\Phi_{in} + \Phi_\infty^i)\rho^i\mathrm{d}^3\mathbf{r} + G_i^0[\rho^i] \qquad \text{where } i = \text{ox, red} \tag{8}$$

Here, the auxiliary charge densities ρ_{in} and ρ_∞^i are in equilibrium with the corresponding polarization potentials Φ_{in} and Φ_∞^i, respectively, and Φ_∞^i is the electronic component of

the total polarization potential, $\Phi^i = \Phi^i_{in} + \Phi^i_\infty$, which is in equilibrium with the charge density ρ^i. The free energy functionals for the reactant and product states in the ET reaction are depicted schematically in Figure 2.

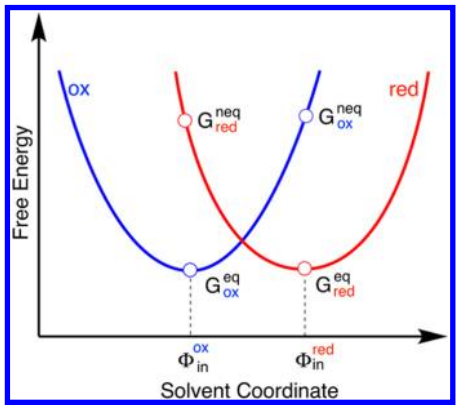

Figure 2. Free energy curves associated with the oxidized (blue) and reduced (red) states of the molecule depicted along the collective solvent coordinate used in Marcus theory for electron transfer. The solute is assumed to remain at a fixed geometry along this collective solvent coordinate. The equilibrium and nonequilibrium free energies used to calculate the solvent reorganization energy are identified on the curves: $G^{eq}_i = G_i[\Phi^i_{in}]$ where i = ox, red and $G^{neq}_i = G_i[\Phi^j_{in}]$ where $i \neq j$.

Within this framework, the state-specific solvent reorganization energies for the oxidized and reduced states are calculated as the differences between nonequilibrium and equilibrium free energies according to the following relations:

$$\lambda_{ox} = G_{ox}[\Phi^{red}_{in}] - G_{ox}[\Phi^{ox}_{in}] = G^{neq}_{ox} - G^{eq}_{ox}$$
$$\lambda_{red} = G_{red}[\Phi^{ox}_{in}] - G_{red}[\Phi^{red}_{in}] = G^{neq}_{red} - G^{eq}_{red} \quad (9)$$

where $G^{eq}_i \equiv G_i[\Phi^i_{in}]$ (i = ox, red) and $G^{neq}_i \equiv G_i[\Phi^j_{in}]$ ($i \neq j$). The solvent reorganization energy λ_s is then given by the average

$$\lambda_s = \frac{1}{2}(\lambda_{ox} + \lambda_{red}) \quad (10)$$

When the charge densities for the solute are computed quantum mechanically by solving the Schrödinger equation with a Hamiltonian that includes the solvent polarization potential in the external potential, the nonequilibrium free energies can be calculated in two distinct limits, as discussed in the next subsection.

B2. Born–Oppenheimer (BO) and Self-Consistent (SC) Limits. The BO and SC limits differ in the treatment of the electronic part of the solvent polarization.[47] In the BO limit, the solvent electrons are assumed to move on a faster time scale than the solute electrons. Therefore, the electronic part of the polarization potential, Φ_∞, retains its equilibrium value Φ^i_∞ corresponding to the equilibrium solute charge density ρ^i of the respective electronic state even when the inertial part of the polarization potential is out of equilibrium. Within this limit, Φ_∞ becomes independent of Φ_{in}, and the free energy functionals have the following form:

$$G^{BO}_i[\Phi_{in}] = -\frac{1}{2}\int \Phi_{in}\rho_{in}\,d^3\mathbf{r} - \frac{1}{2}\int \Phi^i_\infty\rho^i_\infty\,d^3\mathbf{r} + \int (\Phi_{in} + \Phi^i_\infty)\tilde{\rho}^i\,d^3\mathbf{r} + G^0_i[\tilde{\rho}^i] \quad \text{where } i = \text{ox, red} \quad (11)$$

Here, the solute charge density $\tilde{\rho}^i$ corresponds to the wave function Ψ^i obtained by solving the following linear Schrödinger equation:

$$[H^0_i - \Phi_{in} - \Phi^i_\infty]\Psi^i = E\Psi^i \quad \text{where } i = \text{ox, red} \quad (12)$$

where the gas phase Hamiltonian H^0_i corresponds to state i. For simplicity, the Schrödinger equations in this paper are given in atomic units. Note that $\tilde{\rho}^i = \rho^i$ only at equilibrium.

In the SC limit, the solvent electrons are assumed to move on a slower time scale than the transferring electron, and the solvent electronic polarization is equilibrated to the delocalized solute charge distribution. In the framework of dielectric continuum theory, this limit corresponds to the self-consistent treatment of the electronic part of the solvent polarization and the solute charge density. As a result, Φ_∞ is dependent on the solute charge density $\tilde{\rho}^i$, which in turn depends on the total polarization potential $\Phi = \Phi_{in} + \Phi_\infty$. The free energy functionals in the SC limit are given by the following expression:

$$G^{SC}_i[\Phi_{in}] = -\frac{1}{2}\int \Phi_{in}\rho_{in}\,d^3\mathbf{r} - \frac{1}{2}\int \Phi_\infty\tilde{\rho}^i\,d^3\mathbf{r} + \int (\Phi_{in} + \Phi_\infty)\tilde{\rho}^i\,d^3\mathbf{r} + G^0_i[\tilde{\rho}^i] \quad \text{where } i = \text{ox, red} \quad (13)$$

Here, the total charge density $\tilde{\rho}^i$ corresponds to the wave function Ψ^i obtained by solving the following nonlinear Schrödinger equation:

$$[H^0_i - \Phi_{in} - \Phi_\infty(\Psi^i)]\Psi^i = E\Psi^i \quad (14)$$

The difference between eqs 11 and 13 is subtle but important. In the BO limit, the electronic polarization potential is Φ^i_∞, and the density $\tilde{\rho}^i$ is calculated by solving eq 12. In the SC limit, the density $\tilde{\rho}^i$ and electronic polarization potential Φ_∞ must be calculated self-consistently by solving eq 14 and the electrostatic Poisson equation with $\varepsilon = \varepsilon_\infty$ iteratively. In practice, we found that the differences between the reorganization energies calculated in the BO and SC limits are insignificant for the systems studied. For this reason, we present only the results in the SC limit in the main paper and refer the reader to the Supporting Information for a comparison to the results in the BO limit.

The BO and SC approaches represent two opposite limits of a more exact approach that treats the solute and solvent electrons quantum mechanically on the same footing.[45] The BO approach assumes that the solvent electronic polarization responds instantaneously to the pointlike solute electrons. In contrast, the SC approach assumes that the solvent electronic polarization responds much more slowly than the solute electrons and, therefore, is equilibrated to the delocalized solute charge distribution. Typically, the BO approach is more appropriate for electron transfer reactions with weak to modest electronic coupling (i.e., when the electronic coupling is much smaller than the solute–solvent coupling), whereas the SC approach is more appropriate in the opposite regime.[45] In our treatment, the solvent reorganization energy is expressed in terms of the equilibrium and nonequilibrium solvation free

energies corresponding to the diabatic states. Because the electronic characteristics of the diabatic states remain relatively constant and are only weakly dependent on the inertial solvent polarization, the BO and SC approaches are expected to lead to similar solvent reorganization energies, as observed herein.

B3. Implementation in GAMESS. We have implemented a new functionality into the electronic structure program GAMESS[56,57] that enables the calculation of solvent reorganization energies for oxidation and reduction processes using the methodology outlined in the previous subsection. In this subsection, we describe the details of the implementation of this functionality.

In PCM, the solvent polarization is represented by a discrete set of apparent surface charges q_k at the centers of tesserae generated on the surface of a molecular cavity enclosing the solute molecule. The solvent polarization potentials appearing in eqs 11−14 are then expressed in terms of the apparent surface charge density, $\sigma(\mathbf{r}) = \Sigma_k q_k \delta(\mathbf{r} - \mathbf{r}_k)$, represented by the discrete set of apparent surface charges q_k:

$$\Phi(\mathbf{r}) = \int \frac{\sigma(\mathbf{r}')}{|\mathbf{r} - \mathbf{r}'|} \mathrm{d}^2\mathbf{r}' = \sum_k \frac{q_k}{|\mathbf{r} - \mathbf{r}_k|} \tag{15}$$

We also introduce the potential $V(\mathbf{r}')$ induced by the solute charge density $\rho(\mathbf{r})$ on the surface element $\mathbf{r}'$ as the following volume integral:

$$V(\mathbf{r}') = \int \frac{\rho(\mathbf{r})}{|\mathbf{r} - \mathbf{r}'|} \mathrm{d}^3\mathbf{r} \tag{16}$$

The volume integrals appearing in eqs 11 and 13 can be recast as the following surface integrals:

$$\int \Phi(\mathbf{r})\rho(\mathbf{r})\mathrm{d}^3\mathbf{r} = \int \sigma(\mathbf{r}')V(\mathbf{r}')\mathrm{d}^2\mathbf{r}' = \sum_k q_k V_k \tag{17}$$

where the discretized potential is expressed as $V_k = V(\mathbf{r}_k)$.

Using the above definitions, the free energy functionals can be expressed in terms of summations over tesserae to obtain the quantities given in eq 9. Specifically, eq 11 can be expressed as

$$G_i^{\mathrm{BO}}[\Phi_{\mathrm{in}}^j] = -\frac{1}{2}\sum_k q_k^{\mathrm{in},j} V_k^j - \frac{1}{2}\sum_k q_k^{\infty,i} V_k^i + \sum_k (q_k^{\mathrm{in},j} + q_k^{\infty,i})\tilde{V}_k^i + G_i^0[\tilde{\rho}^i]$$

where i, j = ox, red (18)

Here $\tilde{V}_k^i$ is the discretized potential associated with the solute charge density calculated from eq 12. Similarly, eq 13 can be expressed as

$$G_i^{\mathrm{SC}}[\Phi_{\mathrm{in}}^j] = -\frac{1}{2}\sum_k q_k^{\mathrm{in},j} V_k^j - \frac{1}{2}\sum_k \tilde{q}_k^{\infty,i} \tilde{V}_k^i + \sum_k (q_k^{\mathrm{in},j} + \tilde{q}_k^{\infty,i})\tilde{V}_k^i + G_i^0[\tilde{\rho}^i]$$

where i, j = ox, red (19)

Here $\tilde{V}_k^i$ and $\tilde{q}_k^{\infty,i}$ are the discretized potential and apparent surface charges, respectively, associated with the solute charge density and electronic polarization potential Φ_∞, respectively, that are calculated self-consistently via eq 14. In both equations, $q_k^{\infty,i}$ and $q_k^{\mathrm{in},i}$ (i = ox, red) are the apparent surface charges associated with the equilibrium electronic and inertial polarization potentials, respectively, for state i.

The calculation of the solvent reorganization energy as implemented in GAMESS involves a series of calculations of equilibrium and nonequilibrium free energies and is summarized in the flowchart depicted in Figure 3. In the first step, two

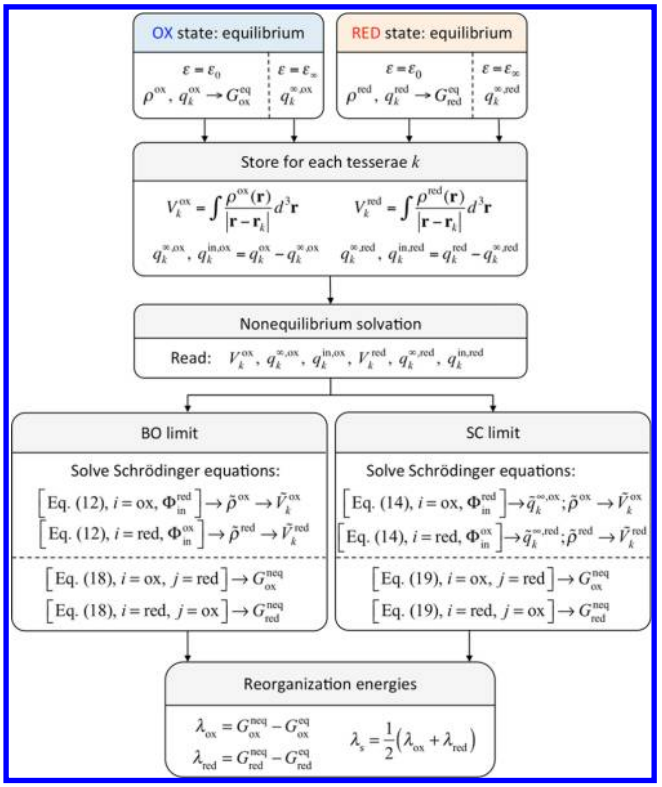

Figure 3. Flowchart illustrating the implementation of the solvent reorganization energy calculation in GAMESS. Note that $G_i^{\mathrm{eq}} \equiv G_i[\Phi_{\mathrm{in}}^i]$ and $G_i^{\mathrm{neq}} \equiv G_i[\Phi_{\mathrm{in}}^j]$, $i \neq j$, where the indices i and j denote the oxidized or reduced state (ox or red). The surface charges associated with Φ_{in}^j are $q_k^{\mathrm{in},j}$, which are fixed, and the surface charges associated with Φ_∞^i are $q_k^{\infty,i}$, which are fixed in the BO limit. In the SC limit, however, the surface charges associated with Φ_∞ are determined iteratively and are denoted $\tilde{q}_k^{\infty,i}$.

sets of equilibrium free energy calculations corresponding to the oxidized and reduced states, respectively, for the solvated molecule at the same solute geometry are performed. Each of the two sets is comprised of two separate free energy calculations with a dielectric constant of ε_0 or ε_∞, respectively. The equilibrium free energies for each state, $G_i^{\mathrm{eq}} \equiv G_i[\Phi_{\mathrm{in}}^i]$ (i = ox, red), where Φ_{in}^i is the equilibrium inertial polarization potential for state i, are obtained directly from the calculation with dielectric constant ε_0. The apparent surface charges q_k are collected for each calculation, and the inertial charges are calculated as the difference between the charges obtained for the total polarization ($\varepsilon = \varepsilon_0$) and the electronic polarization ($\varepsilon = \varepsilon_\infty$). The equilibrium solute charge densities ρ^i (i = ox, red) determined with dielectric constant ε_0 are converted to discretized potentials V_k^i according to eq 16. The apparent surface charges $q_k^{\infty,i}$ and $q_k^{\mathrm{in},i}$ and the discretized potentials V_k^i are stored for each state i = ox, red.

For the nonequilibrium calculations, the free energy for state i, denoted G_i, is calculated at the equilibrium inertial polarization potential for the complementary state j, denoted

dx.doi.org/10.1021/ct500051e | J. Chem. Theory Comput. 2014, 10, 2091−2102

Φ^j_{in}, thereby providing $G^{neq}_i \equiv G_i[\Phi^j_{in}]$. In the BO limit (eqs 11 and 12), the solute charge density is equilibrated with the total nonequilibrium polarization potential $\Phi^j_{in} + \Phi^i_\infty$, whereas in the SC limit (eqs 13 and 14), the solute charge density and Φ_∞ are determined iteratively while keeping the inertial solvent polarization potential Φ^j_{in} fixed. The solute charge density obtained from either one of these procedures is converted to the discretized potential $\tilde{V}^i_k$. The surface charges associated with Φ^j_{in} are $q^{in,j}_k$, which are fixed, and the surface charges associated with Φ^i_∞ are $q^{\infty,i}_k$, which are fixed in the BO limit. In the SC limit, however, the surface charges associated with Φ_∞ are determined iteratively and are denoted as $\tilde{q}^{\infty,i}_k$. All of these quantities can be used to calculate the free energies given by eq 18 or eq 19 in the BO or SC limit, respectively. After completion of these calculations, the solvent reorganization energy is obtained as the difference between the nonequilibrium and equilibrium free energies, as given in eq 9.

When calculating the solvent reorganization energy independently of the inner-sphere reorganization energy, the geometry of the molecule remains fixed. In other words, the solvent reorganization is assumed to be associated with only the changes in the inertial solvent polarization potential (i.e., the solvent coordinate in Figure 2). As a result of this construct, the solvent reorganization energy needs to be calculated for the two different geometries corresponding to the optimized equilibrium geometries of the oxidized and reduced species. The resulting solvent reorganization energies are averaged to obtain the total solvent reorganization energy for the system. We have found that the solvent reorganization energies for the two different geometries are nearly identical for the systems studied.

C. Effects of Electrode. The original formulation of PCM for a homogeneous dielectric medium, also referred to as dielectric PCM (DPCM), has been extended to describe inhomogeneous media consisting of multiple dielectrics.[58−61] In this formulation, the boundary conditions for each interface between media with different dielectric constants are treated explicitly. An alternative approach utilizes the IEF-PCM formalism, in which the solute−solvent boundary is treated explicitly, and the effects of other boundaries are included through an external Green's function and its normal derivative.[62,63] The IEF-PCM equations can be solved either iteratively[64,65] or by matrix inversion.[55]

Our approach is based on the matrix-inversion formulation of the IEF-PCM, as implemented in GAMESS. In this approach, the surface charge density $\sigma(\mathbf{r})$, which is represented as a vector $\boldsymbol{\sigma}$ with components equal to the apparent surface charges at the centers of the tesserae, is obtained as a solution of the following matrix equation:

$$\mathbb{C}\boldsymbol{\sigma} = -\mathbf{V} \tag{20}$$

Here, the vector $\mathbf{V}$ has components equal to the electrostatic potential at the center of each tessera induced by the solute charge density. The matrix $\mathbb{C}$ is given by the following expression:

$$\mathbb{C} = \left[\left(\frac{\mathbb{A}}{2} - \mathbb{D}^E\right) - \mathbb{S}^E(\mathbb{S}^I)^{-1}\left(\frac{\mathbb{A}}{2} - \mathbb{D}^I\right)\right]^{-1} 4\pi\left[\mathbb{S}^E\mathbb{A}^{-1}\left(\frac{\mathbb{A}}{2} + \mathbb{D}^{I*}\right) + \left(\frac{\mathbb{A}}{2} - \mathbb{D}^E\right)\mathbb{A}^{-1}\mathbb{S}^I\right] \tag{21}$$

In this expression, the matrices $\mathbb{S}^I$ and $\mathbb{S}^E$ are related to the Green's functions inside and outside of the cavity, respectively; the matrices $\mathbb{D}^I$ and $\mathbb{D}^E$ are related to the normal derivatives of the Green's functions, respectively; and $\mathbb{A}$ is the diagonal matrix with diagonal components equal to the areas of the tesserae. The definition of the matrix $\mathbb{C}$ given in eq 21 is general and can be used for both homogeneous (i.e., single dielectric) and inhomogeneous (i.e., multiple dielectrics) media. Note that the IEF formalism implicitly accounts for the effects of escaped charges.[66−68]

With the use of suitable Green's functions, eq 21 can be utilized to compute the apparent surface charges for dielectric media in the presence of an electrode. Although the Green's function inside the cavity remains unaffected by the presence of an electrode, the external Green's function should reflect its presence. When the electrode is treated as a perfect conductor with dielectric constant $\varepsilon = \infty$, the external Green's function $G^E(\mathbf{r}, \mathbf{r}')$ includes the contribution from the image charges and is given by the following expression:

$$G^E(\mathbf{r}, \mathbf{r}') = \frac{1}{\varepsilon}\left(\frac{1}{|\mathbf{r} - \mathbf{r}'|} - \frac{1}{|\mathbf{r} - \mathbf{M}(\mathbf{r}')|}\right) \tag{22}$$

where ε is the solvent dielectric constant and $\mathbf{M}(\mathbf{r}')$ is the mirror image of the vector $\mathbf{r}'$ with respect to the electrode surface. Using this definition of the external Green's function, the matrix elements of the matrices $\mathbb{S}$ and $\mathbb{D}$ in eq 21 are given by the following explicit expressions,[69] which are valid for the tessellation scheme GEPOL-GB[70] implemented in GAMESS:

$$S^I_{ii} = 1.07a_i\sqrt{\frac{a_i}{4\pi}} \qquad S^I_{ij} = \frac{a_i a_j}{4\pi|\mathbf{r}_i - \mathbf{r}_j|} \qquad \text{where } i \neq j \tag{23}$$

$$D^I_{ii} = -\frac{S^I_{ii}}{2R_i} \qquad D^I_{ij} = \frac{a_i a_j(\mathbf{r}_i - \mathbf{r}_j)\mathbf{n}_j}{4\pi|\mathbf{r}_i - \mathbf{r}_j|^3} \qquad \text{where } i \neq j \tag{24}$$

$$S^E_{ij} = \frac{1}{\varepsilon}\left(S^I_{ij} - \frac{a_i a_j}{4\pi|\mathbf{r}_i - \mathbf{M}(\mathbf{r}_j)|}\right) \tag{25}$$

$$D^E_{ij} = D^I_{ij} - \frac{a_i a_j[\mathbf{r}_i - \mathbf{M}(\mathbf{r}_j)]\mathbf{n}_j}{4\pi|\mathbf{r}_i - \mathbf{M}(\mathbf{r}_j)|^3} \tag{26}$$

where a_i is the area of the ith tessera, R_i is the radius of the sphere on which the ith tessera is located, and $\mathbf{n}_i$ is the unit vector normal to the surface of the ith tessera.

We have implemented this IEF-PCM approach in the electronic structure program GAMESS.[56,57] In the current formulation, the surface charges are generated using the total potential (i.e., the sum of the electronic and nuclear potential energy contributions) to keep the energy expressions similar to the iterative procedure already implemented for the calculation of homogeneous free energies. The matrix $\mathbb{C}$ in eq 21 is computed twice, first using the static dielectric constant ε_0 and subsequently using the optical dielectric constant ε_∞. These matrices are then utilized to calculate the surface charges due to the total and electronic responses of the solvent polarization. The difference between these two sets of surface charges results in the surface charges due to the inertial response of the solvent. The reorganization energies are subsequently computed using the procedure described in section B3.

D. Connection to Experiment. Connecting calculated reorganization energies to experimentally measured properties

is challenging because reorganization energies are difficult to measure directly. For this reason, other observable quantities are often measured instead, and the reorganization energy is extracted from these data. Moreover, the measured values are obtained for a specific set of experimental conditions, such as temperature, electrolyte type and concentration, electrode type, solute, and solvent. A complete understanding of the relations among these properties requires knowledge of the double layer characteristics, which are related to the structure of the environment (i.e., the electrolyte, solute, and solvent) at and near the surface of the electrode. Thus, a molecular description of the interface may be required for a quantitative description of electrocatalytic reactions.[71−73]

In the framework of the Guoy−Chapman−Stern (GCS) model[74,75] for the double layer and in the limit of low electrolyte concentrations, the current density in the electrochemical reduction/oxidation process is dominated by the ET reaction occurring at the distance of closest approach to the electrode surface, the so-called reaction plane (RP) distance. In the absence of specific adsorption of electrolyte ions, the RP is usually associated with the outer Helmholtz plane (OHP), which is identified with the ordered layer of solvated electrolyte ions on top of the layer of solvent molecules adsorbed on the surface of the electrode. In the specific case of large electrolyte ions, however, the RP can also be associated with the inner Helmholtz plane (IHP), which is identified with a single layer of adsorbed solvent molecules.

In the following calculations, we considered both scenarios, depending on the structure of the solute molecule. In the case of nonplanar solute molecules, the RP was assumed to be associated with the OHP. For planar molecules, two separate calculations were performed with the solute placed at the OHP or the IHP. The distance to the OHP from the electrode surface was calculated as the sum of the diameter of the solvent molecule, D_{solv}, and the solvated radius of the electrolyte ion, R_{ion}:[74,76,77]

$$d_{OHP} = D_{solv} + R_{ion} \tag{27}$$

The distance to the IHP from the electrode surface was determined from the diameter of the solvent molecule: $d_{IHP} = D_{solv}$.

The Frumkin correction accounts for the effects of the double layer on the ET rate constant.[78,79] It relates the apparent (i.e., experimentally measured) ET standard rate constant k_s^{app}, which depends on the potential induced by the double layer and supporting electrolyte, to the "true" ET standard rate constant k_s^{true}. The relation is given by the following expression:[74,80−84]

$$k_s^{true} = k_s^{app}\exp\left[-\frac{(\alpha n - z)F\phi^d}{RT}\right] \tag{28}$$

where ϕ^d is the electrostatic potential at the reaction plane relative to the potential in the bulk solvent, α is the transfer coefficient, n is the number of electrons transferred, z is the total charge of the oxidized species, F is the Faraday constant, R is the universal gas constant, and T is the temperature. The exponential term in eq 28 is related to the electrostatic work required to bring the solute species from the bulk solvent to the reaction plane.

To express the total reorganization energy, λ_{tot}, in terms of the activation free energy, $\Delta G^{\ddagger,true}$, corresponding to the "true" rate constant k_s^{true}, we use the standard Marcus expression for electrochemical ET. This expression relates the activation free energy to the total reorganization energy and the applied overpotential η

$$\Delta G^{\ddagger,true}(\eta) = \frac{(\lambda_{tot} + \eta)^2}{4\lambda_{tot}} \tag{29}$$

For simplicity, we neglect the temperature-dependent entropic contributions to the activation free energy and, therefore, assume that $\Delta G^{\ddagger,true} \approx \Delta H^{\ddagger,true}$. In this case, noting that the standard rate constants are defined at zero overpotential, $\eta = 0$, we can express the reorganization energy λ_{tot} in terms of the activation enthalpy $\Delta H_s^{\ddagger,true}$, where the subscript "s" signifies that this quantity corresponds to the standard rate constant:

$$\lambda_{tot} = 4\Delta H_s^{\ddagger,true} \tag{30}$$

To relate the reorganization energy to the measured (apparent) standard rate constant, we differentiate the logarithm of eq 28, as well as the relation $k_s^{true} \propto \exp(-\Delta H^{\ddagger,true}/(RT))$, with respect to the inverse temperature and obtain

$$\frac{\partial(\ln k_s^{true})}{\partial(1/T)} = -\frac{\Delta H_s^{\ddagger,true}}{R} = \frac{\partial(\ln k_s^{app})}{\partial(1/T)} - \frac{F(\alpha n - z)}{R}\frac{\partial(\phi^d/T)}{\partial(1/T)} \tag{31}$$

Finally, using eq 30, we obtain

$$\lambda_{tot} = -4R\frac{\partial(\ln k_s^{app})}{\partial(1/T)} + 4F(\alpha n - z)\frac{\partial(\phi^d/T)}{\partial(1/T)} \tag{32}$$

In some cases, the experimental values reported have already been corrected for these effects, and we can directly compare the calculated and experimentally determined reorganization energies. In other cases, however, eq 32 must be used to relate the experimental values to the calculated values. The use of eq 32 requires knowledge of the temperature dependence of ϕ^d, which can be related to experimentally measurable quantities using Guoy−Chapman Theory.[85−87] If the charge density at the electrode surface is sufficiently large, the quantity $\partial(\phi^d/T)/\partial(1/T)$ approaches zero and can be neglected.[88] Thus, in the following analysis, we compare the calculated values of the reorganization energies with the reorganization energies extracted from the standard apparent rate constants, k_s^{app}:

$$\lambda_{tot}^{expt} = 4\Delta H_s^{\ddagger,app} \tag{33}$$

E. Computational Details. In our calculations, we used density functional theory (DFT) with a modified version of the B3LYP functional,[89,90] implemented in GAMESS as B3LYPV3, where the electron gas formula 3 of VWN correlation has been used,[91,92] and the 6-31G** basis set.[93,94] The free energies of the solvated molecules and the solvent reorganization energies were calculated using the IEF-PCM approach. The dielectric constants of the solvents are given in Table S1 of the Supporting Information. The discretization of the solute surface utilized the GEPOL-GB tessellation scheme,[70] and the simplified united atom Hartree−Fock (SUAHF) radii were used to generate the molecular cavity.[95] The radii of the solvent molecules and the solvated electrolyte ions, Bu_4N^+ or Et_4N^+,[96] were used to obtain an estimate for the thickness of the OHP according to eq 27 and are given in Tables S1 and S2 of the Supporting Information. For the calculation of solvent reorganization energies using the Marcus point-charge model,

the effective radius of the sphere was estimated by equating the volume of the sphere to the volume of the cavity generated in the IEF-PCM calculation. The choice of the radius for the model involving a collection of atomic charges is slightly more involved and is described in the Supporting Information.

The calculated value of the electrochemical reorganization energy also depends on the orientation of the molecule relative to the electrode surface. In principle, the reorganization energy should be calculated with a Boltzmann averaging procedure for different orientations. However, as discussed in the next section, the dependence of the solvent reorganization energy on molecular orientation is found to be very weak for the systems studied, and thus, the averaging procedure was not used in the reported calculations.

3. RESULTS AND DISCUSSION

We applied the methodology described in the previous section to the set of representative molecules shown in Figure 4. The

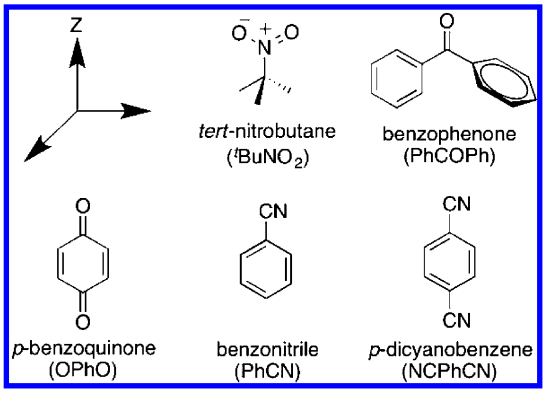

Figure 4. Molecules for which the reorganization energies were calculated and compared to experimental values.

nonplanar molecules were oriented such that the electrode surface was placed perpendicular to the z-axis according to the orientation depicted in Figure 4. For the planar molecules, we considered the two geometries corresponding to the molecular plane parallel or perpendicular to the electrode surface. As mentioned above, the distance d from the center of mass of the molecule to the electrode surface was chosen to be the distance to the OHP. For planar molecules, however, we also provide the values for the molecules located at the IHP because planar molecules are expected to be able to move closer to the electrode when the molecular plane is parallel to the electrode surface.

Table 1 compares the calculated total reorganization energies for these molecules with the experimentally measured values, λ_{tot}^{expt}, in a variety of solvents and supporting electrolytes. This table provides the inner-sphere reorganization energies, λ_i, as well as the total reorganization energies obtained from the sum of the inner-sphere reorganization energy and the solvent reorganization energy calculated with three different approaches: λ_{tot}^{pc}, the Marcus point-charge model with the electrode, given by eq 5; λ_{tot}^{iso}, the isotropic PCM approach, which does not include the effects of the electrode; and λ_{tot}^{echem}, the IEF-PCM approach, which includes the effects of the electrode. As mentioned above, we extended the Marcus point-charge model to a collection of point charges corresponding to the atomic partial charges of the molecule. As shown in Table S3 of the Supporting Information, the solvent reorganization energies obtained with the collection of point charges are nearly identical to those obtained with a single point charge provided the radius of the surrounding sphere is the same. Specifically, the differences were less than ~2 kcal/mol for all cases studied. The IEF-PCM calculations were performed with both the BO and the SC methods for the treatment of the electronic part of the solvent polarization. As shown in Tables S4 and S5 of the Supporting Information, these two methods lead to solvent reorganization energies that differ by less than 0.05 kcal/mol.

We investigated the impact of molecular orientation and geometry of the solute on the solvent reorganization energies. Table 1 presents the results with the molecular planes of the planar molecules parallel to the electrode surface. The results for the perpendicular orientations are given in Table 2 and illustrate that the solvent reorganization energy is relatively insensitive to this orientation. Specifically, Table 2 indicates that the reorganization energies for the parallel and perpendicular orientations differ by less than ~0.3 kcal/mol in all cases studied. Thus, although in principle, the results could be averaged over a Boltzmann distribution of molecular orientations, they do not depend significantly on this property. In addition, the solvent reorganization energies given in Table 1 were calculated as the average of the values obtained for the equilibrium geometries corresponding to the oxidized and reduced states of the molecules. As shown in Table S6 in the Supporting Information, the solvent reorganization energy is relatively insensitive to these geometrical differences. In particular, the reorganization energies calculated with the geometries of the oxidized and reduced species differ by less than ~0.2 kcal/mol in all cases studied. Thus, this approximation appears to have a negligible effect.

Overall, the agreement between the calculated and experimental reorganization energies is very reasonable when the effects of the electrode are included in the calculations. Moreover, if the distance between the electrode and the molecule is fixed, the reorganization energy decreases as the static dielectric constant of the solvent decreases. Supporting Information Table S7 provides a comparison of the different components of the free energy functional in eq 19 for the oxidized geometry of *p*-dicyanobenzene in acetonitrile and dichloromethane solvents. The main difference between the reorganization energies in the two solvents arises from the first term of eq 19 for the nonequilibrium free energy; this term represents the nonequilibrium self-energy of the inertial component of the solvent polarization.

According to Marcus theory, the intrinsic free energy barrier for electron transfer is $\lambda/4$.[97] Thus, errors of ~4 kcal/mol in λ lead to ~1 kcal/mol error in free energy barrier, corresponding to less than 1 order of magnitude in the rate constant at room temperature. For all molecules studied, the isotropic PCM approach significantly overestimates the solvent reorganization energies, illustrating that the effects of the electrode are important and therefore are essential to include in the calculations. Moreover, in all cases, the Marcus point-charge model and the IEF-PCM approach, which both include the effects of the electrode, agree well with each other. For the nonplanar molecules placed at the OHP, both the Marcus point-charge model and the IEF-PCM approach agree well with the experimental values. For the planar molecules, the agreement is much better when the molecule is placed at the IHP, consistent with the proposal that planar molecules tend to be closer to the electrode. Figure 5 depicts the dependence of the calculated electrochemical solvent reorganization energy on

Table 1. Comparison of Calculated Total Reorganization Energies with Experimental Values for Various Molecules in Different Solvents[a]

solute	solvents[b]	electrolyte[c]	d (Å)	λ_i[d]	λ_{tot}^{pc}[e]	λ_{tot}^{iso}[f]	λ_{tot}^{echem}[g]	λ_{tot}^{expt}[h]
$^tBuNO_2$[i]	DMF	0.1 TBAP	10.03	19.92	40.64	45.89	41.99	40.13[98]
PhCOPh[i]	DMSO	0.1 TEAP	8.91	4.84	20.65	23.76	19.76	22.94[99]
	DMA	0.1 TEAP	9.37	4.84	21.57	24.54	20.58	22.08[99]
OPhO[j]	DMF	0.1 TEAP	4.91	5.85	22.94	29.72	21.52	25.27[100]
			8.91	5.85	26.45	29.72	25.47	
	ACN	0.1 TEAP	4.31	5.85	24.05	32.88	21.96	22.97[100]
			8.31	5.85	28.92	32.88	27.69	
PhCN[j]	DMF	0.1 TBAP	4.91	4.44	21.27	27.62	19.06	20.27[101]
			10.03	4.44	25.25	27.62	23.84	
NCPhCN[j]	DMF	0.1 TBAP	4.91	4.05	19.22	25.63	18.49	19.89[102]
			10.03	4.05	23.21	25.63	21.99	
	ACN	0.1 TBAP	4.31	4.05	20.07	28.46	19.40	17.69[102]
			9.45	4.05	25.58	28.46	24.10	
	ATO	0.1 TBAP	4.76	4.05	20.04	27.02	19.21	14.34[102]
			9.91	4.05	24.53	27.02	23.10	
	DCM	0.1 TBAP	4.54	4.05	16.11	21.80	15.50	14.91[102]
			9.54	4.05	19.78	21.80	18.65	

[a]All reorganization energy values given in units of kilocalories per mole. For each solute, the solvents are arranged in decreasing order of static dielectric constant. [b]DMF = dimethylformamide; DMA = dimethylacetamide; DMSO = dimethylsulfoxide; ACN = acetonitrile; ATO = acetone; DCM = dichloromethane. [c]TBAP = tetrabutylammonium perchlorate; TEAP = tetraethylammonium perchlorate. [d]Calculated inner-sphere reorganization energy. [e]Total reorganization energy with the solvent reorganization energy calculated analytically with point charge and electrode. [f]Total reorganization energy with the solvent reorganization energy calculated isotropically without electrode. [g]Total reorganization energy with the solvent reorganization energy calculated electrochemically with electrode. [h]Experimental values obtained from the references cited. [i]Solute molecule positioned at the OHP. [j]The planar molecules (OPhO, PhCN, NCPhCN) are positioned parallel to the electrode at the IHP (first entry) or at the OHP (second entry). In most cases, the results agree better with the experimental values when the molecule is at the IHP than at the OHP because planar molecules are expected to be located closer to the electrode surface.

Table 2. Calculated Total Reorganization Energies at Two Different Orientations of the Planar Molecules Relative to the Electrode, Maintaining a Constant Distance between the Center of Mass and the Electrode Surface

			λ_{tot}^{echem}[b]	
solutes	solvents[a]	d (Å)	$\parallel$[c]	$\perp$[d]
OPhO	DMF	8.91	25.47	25.47
	ACN	8.31	27.69	27.69
PhCN	DMF	10.03	23.84	23.84
NCPhCN	DMF	10.03	21.99	21.82
	ACN	9.45	24.10	23.85
	ATO	9.91	23.10	22.89
	DCM	9.54	18.65	18.46

[a]DMF = dimethylformamide; ACN = acetonitrile; ATO = acetone; DCM = dichloromethane. [b]Total reorganization energy in kilocalories per mole with solvent reorganization energy calculated electrochemically with electrode. [c]Electrode surface is parallel to the molecular plane. [d]Electrode surface is perpendicular to the molecular plane.

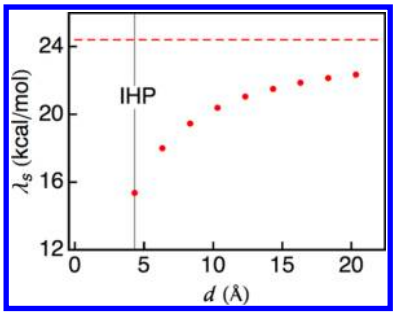

Figure 5. Dependence of the electrochemical solvent reorganization energy on the distance d between the molecule and the electrode surface for *p*-dicyanobenzene (NCPhCN), where the molecule is oriented parallel to the electrode surface. The first point corresponds to the distance associated with the IHP. Only the solvent reorganization energy is shown because the inner-sphere reorganization energy is independent of this distance. The dashed line corresponds to the isotropic solvent reorganization energy without including the effects of the electrode.

the distance between the molecule and the electrode surface. As this distance increases, the electrochemical reorganization energy approaches the isotropic value, indicated by the horizontal line in Figure 5.

4. CONCLUDING REMARKS

In this paper, we presented a computational method for calculating the electrochemical solvent reorganization energy for electron transfer reactions. This approach separates the electronic and inertial responses of the solvent according to their respective time scales and includes the boundary effects associated with the molecular-shaped cavity in solution and at the electrode−solution interface. Thus, this method accounts for the effects of the detailed molecular charge redistribution in a molecular-shaped cavity, as well as the electronic and inertial solvent responses and the effects of the electrode on electron transfer. Inclusion of the effects of the electrode is found to be essential for obtaining even qualitatively accurate solvent reorganization energies. The results obtained from this approach are similar to those obtained from a simple point-charge model that also includes the effects of the electrode. The results from both of these approaches are in reasonable agreement with experimentally measured values.

We emphasize that the similarity between the IEF-PCM method and the point-charge model may be due to the simplicity of the molecules studied and may not extend to

dx.doi.org/10.1021/ct500051e | J. Chem. Theory Comput. 2014, 10, 2091−2102

larger, more complex systems. Nevertheless, these results suggest that the main properties determining the solvent reorganization energy for these systems are the volume of the cavity, the change in overall solute charge (i.e., the number of electrons transferred), and the distance of the molecule from the electrode surface. Although the cavity volume is critical, the specific shape is not crucial, so similar results are obtained for spherical and molecular-shaped cavities of equal volume. Similarly, although the change in overall charge of the solute is paramount, the specific distribution of the electronic charge within the cavity is not significant. Thus, similar results are obtained when all of the charge is placed at the center of the cavity compared to the more realistic molecular charge distribution obtained from electronic structure calculations.

We have also found that the results are not sensitive to the details of the molecular geometry (i.e., reduced or oxidized state geometries) or the molecular orientation. However, the distance between the molecule and the electrode surface strongly impacts the solvent reorganization energy. If the distance distribution function of the molecule with respect to the electrode surface were available, a series of solvent reorganization energy calculations could be performed at a range of distances, and the overall solvent reorganization energy could be determined by weighting these values according to the distribution function. Such information about the distribution function could be obtained from molecular dynamics simulations with explicit solvent molecules and electrolyte ions at an electrode surface.

This method can be extended to provide a more accurate representation of experimentally relevant electrochemical systems. The Green's functions can be modified to include additional regions with specified dielectric constants. For example, a self-assembled monolayer tethering the molecule to the electrode can be described in terms of a region with a distinct dielectric constant. The double layer effects associated with the solvent and electrolyte ions at the interface can also be described in this manner. Explicit molecular dynamics simulations of the solvent/electrode interface could be performed to provide information about the structure of the solvent and ions in this interfacial region. Such information could be used to develop more elaborate models for calculating the electrochemical solvent reorganization energies. Moreover, the calculated reorganization energies can be used to determine rate constants for electron transfer at electrochemical interfaces. Feedback between the calculations and experimental measurements will guide the improvement of the computational methods, as well as the characterization and understanding of complex electrochemical systems. Such insights will have implications for the design of more effective molecular electrocatalysts.

APPENDIX

In this Appendix, we present the expression for the average potential on the surface of a sphere due to a point charge at the center of a sphere (Figure 1). In spherical coordinates with the origin at the center of the sphere with radius a, the average potential $\bar{\phi}$ is given by the following expression:

$$\bar{\phi} = \frac{1}{4\pi a^2} \cdot a^2 \int_0^{2\pi} d\varphi \int_0^{\pi} d\theta \sin\theta \, \phi(a, \theta, \varphi) \tag{A1}$$

In the case of a single point charge at a distance d from the metal electrode surface, the electrostatic potential $\phi(a, \theta, \varphi)$ at a point with spherical angles (θ, φ) on the surface of a sphere is independent of φ due to azimuthal symmetry of the system. This electrostatic potential is obtained as a solution of the Poisson equation given in eq 2. In cylindrical coordinates (ρ, z, φ), the solution is given by the following expression:

$$\phi(\rho, z) = \frac{\Delta q}{\varepsilon}\left[\frac{1}{(\rho^2 + z^2)^{1/2}} - \frac{1}{(\rho^2 + (2d - z)^2)^{1/2}}\right] \tag{A2}$$

which can be converted to spherical coordinates using the standard relations

$$\rho^2 = a^2 \sin^2\theta \qquad z = a\cos\theta \qquad \rho^2 + z^2 = a^2 \tag{A3}$$

The final form of the electrostatic potential in spherical coordinates is given by

$$\phi(a, \theta) = \frac{\Delta q}{\varepsilon}\left[\frac{1}{a} - \frac{1}{(a^2 - 4da\cos\theta + 4d^2)^{1/2}}\right] \tag{A4}$$

Finally, the average potential can be calculated analytically by evaluating the double integral in eq A1 to obtain the result given in eq 4 of the main text. The analogous equations for a collection of partial atomic charges inside the sphere are given in the Supporting Information.

ASSOCIATED CONTENT

Supporting Information

Solvent and electrolyte properties; description and comparison of models with a single point charge and a collection of atomic charges in a sphere near an electrode; comparison of reorganization energies in Born−Oppenheimer and self-consistent limits for isotropic and electrochemical methods; comparison of reorganization energies for oxidized and reduced state geometries; comparison of components of free energy functionals for the oxidized geometry of *p*-dicyanobenzene in acetonitrile and dichloromethane; coordinates of optimized geometries for all molecules studied. This material is available free of charge via the Internet at http://pubs.acs.org.

AUTHOR INFORMATION

Corresponding Author

*S. Hammes-Schiffer. E-mail: shs3@illinois.edu.

Present Address

[†]Illinois Rocstar LLC, 1800 South Oak Street, Suite 208, Champaign, Illinois 61820, United States.

Author Contributions

[‡]These authors contributed equally to this paper.

Funding

This research was supported as part of the Center for Molecular Electrocatalysis, an Energy Frontier Research Center funded by the U.S. Department of Energy, Office of Science, Office of Basic Energy Sciences.

Notes

The authors declare no competing financial interest.

ACKNOWLEDGMENTS

We would like to thank Daniel Chipman and Benedetta Mennucci for their helpful scientific discussions and insights. We would also like to thank Hui Li for his expertise in the PCM implementation in GAMESS.

REFERENCES

(1) Akimov, A. V.; Neukirch, A. J.; Prezhdo, O. V. *Chem. Rev.* **2013**, *113*, 4496−4565.
(2) Mohamed, H. H.; Bahnemann, D. W. *Appl. Catal., B* **2012**, *128*, 91−104.
(3) Ai, X.; Lian, T. Ultrafast photoinduced interfacial electron transfer dynamics in molecule-inorganic semiconductor nanocomposites. *Funct. Nanomat.* **2006**, 301.
(4) Meyer, G. J. *Inorg. Chem.* **2005**, *44*, 6852−6864.
(5) Zhang, J.; Chi, Q.; Albrecht, T.; Kuznetsov, A. M.; Grubb, M.; Hansen, A. G.; Wackerbarth, H.; Welinder, A. C.; Ulstrup, J. *Electrochim. Acta* **2005**, *50*, 3143−3159.
(6) Durrant, J. R.; Haque, S. A.; Palomares, E. *Coord. Chem. Rev.* **2004**, *248*, 1247−1257.
(7) Hagfeldt, A.; Graetzel, M. *Chem. Rev.* **1995**, *95*, 49−68.
(8) Marcus, R. A. *J. Chem. Phys.* **1965**, *43*, 679−701.
(9) Smith, B. B.; Hynes, J. T. *J. Chem. Phys.* **1993**, *99*, 6517−6530.
(10) Hush, N. S. *J. Electroanal. Chem.* **1999**, *470*, 170−195.
(11) Kuznetsov, A. M. *Charge Transfer in Physics, Chemistry and Biology*; CRC Press: Boca Raton, FL, 1995.
(12) Royea, W. J.; Fajardo, A. M.; Lewis, N. S. *J. Phys. Chem. B* **1997**, *101*, 11152−11159.
(13) Chidsey, C. E. D. *Science* **1991**, *251*, 919−922.
(14) Zusman, L. D. *Chem. Phys.* **1987**, *112*, 53−59.
(15) Hashino, T. *J. Chem. Phys.* **1967**, *46*, 4639−4645.
(16) Marcus, R. A. *J. Phys. Chem.* **1963**, *67*, 853−857.
(17) Marcus, R. A. *Can. J. Chem.* **1959**, *37*, 155−163.
(18) Marcus, R. A. *Annu. Rev. Phys. Chem.* **1964**, *15*, 155−196.
(19) Klimkāns, A.; Larsson, S. *Chem. Phys.* **1994**, *189*, 25−31.
(20) Liu, Y.-P.; Newton, M. D. *J. Phys. Chem.* **1994**, *98*, 7162−7169.
(21) Liu, Y.-P.; Newton, M. D. *J. Phys. Chem.* **1995**, *99*, 12382−12386.
(22) Caricato, M.; Ingrosso, F.; Mennucci, B.; Sato, H. *J. Phys. Chem. B* **2006**, *110*, 25115−25121.
(23) Zhou, Z.; Khan, S. U. M. *J. Phys. Chem.* **1989**, *93*, 5292−5295.
(24) Mikkelsen, K. V.; Pedersen, S. U.; Lund, H.; Swanstroem, P. *J. Phys. Chem.* **1991**, *95*, 8892−8899.
(25) Jakobsen, S.; Mikkelsen, K. V.; Pedersen, S. U. *J. Phys. Chem.* **1996**, *100*, 7411−7417.
(26) Basilevsky, M. V.; Chudinov, G. E.; Rostov, I. V.; Liu, Y.-P.; Newton, M. D. *J. Mol. Struct.: THEOCHEM* **1996**, *371*, 191−203.
(27) Newton, M. D.; Basilevsky, M. V.; Rostov, I. V. *Chem. Phys.* **1998**, *232*, 201−210.
(28) Zichi, D. A.; Ciccotti, G.; Hynes, J. T.; Ferrario, M. *J. Phys. Chem.* **1989**, *93*, 6261−6265.
(29) Van Voorhis, T.; Kowalczyk, T.; Kaduk, B.; Wang, L.-P.; Cheng, C.-L.; Wu, Q. *Annu. Rev. Phys. Chem.* **2010**, *61*, 149−170.
(30) Hartnig, C.; Koper, M. T. M. *J. Chem. Phys.* **2001**, *115*, 8540−8546.
(31) Warshel, A.; Parson, W. W. *Annu. Rev. Phys. Chem.* **1991**, *42*, 279−309.
(32) Matyushov, D. V. *J. Chem. Phys.* **2004**, *120*, 7532−7556.
(33) Tanimura, Y.; Leite, V. B. P.; Onuchic, J. N. *J. Chem. Phys.* **2002**, *117*, 2172−2179.
(34) Leontyev, I. V.; Basilevsky, M. V.; Newton, M. D. *Theor. Chem. Acc.* **2004**, *111*, 110−121.
(35) Leontyev, I. V.; Tachiya, M. *J. Chem. Phys.* **2005**, *123*, 224502.
(36) Bader, J. S.; Cortis, C. M.; Berne, B. J. *J. Chem. Phys.* **1997**, *106*, 2372−2387.
(37) Leontyev, I. V.; Tachiya, M. *J. Chem. Phys.* **2007**, *126*, 064501.
(38) Domínguez-Ariza, D.; Hartnig, C.; Sousa, C.; Illas, F. *J. Chem. Phys.* **2004**, *121*, 1066−1073.
(39) Hartnig, C.; Koper, M. T. M. *J. Am. Chem. Soc.* **2003**, *125*, 9840−9845.
(40) Kuznetsov, A. M.; Schmickler, W. *Chem. Phys. Lett.* **2000**, *327*, 314−318.
(41) Sebastian, K. L. *J. Chem. Phys.* **1989**, *90*, 5056−5067.
(42) Boroda, Y. G.; Voth, G. A. *J. Electroanal. Chem.* **1998**, *450*, 95−107.
(43) Basilevsky, M. V.; Chudinov, G. E.; Newton, M. D. *Chem. Phys.* **1994**, *179*, 263−278.
(44) Jackson, J. D. *Classical Electrodynamics*, 3rd ed.; Wiley: Hoboken, NJ, 1998.
(45) Kim, H. J.; Hynes, J. T. *J. Chem. Phys.* **1992**, *96*, 5088−5110.
(46) Cossi, M.; Barone, V. *J. Phys. Chem. A* **2000**, *104*, 10614−10622.
(47) Basilevsky, M. V.; Chudinov, G. E.; Napolov, D. V. *J. Phys. Chem.* **1993**, *97*, 3270−3277.
(48) Mathis, J. R.; Bianco, R.; Hynes, J. T. *J. Mol. Liq.* **1994**, *61*, 81−101.
(49) Gehlen, J. N.; Chandler, D.; Kim, H. J.; Hynes, J. T. *J. Phys. Chem.* **1992**, *96*, 1748−1753.
(50) Marcus, R. A. *J. Phys. Chem.* **1992**, *96*, 1753−1757.
(51) Born, M. *Z. Phys.* **1920**, *1*, 45−48.
(52) Ayala, R.; Sprik, M. *J. Phys. Chem. B* **2007**, *112*, 257−269.
(53) Basilevsky, M. V.; Chudinov, G. E. *Chem. Phys.* **1991**, *157*, 327−344.
(54) Miertuš, S.; Scrocco, E.; Tomasi, J. *Chem. Phys.* **1981**, *55*, 117−129.
(55) Tomasi, J.; Mennucci, B.; Cammi, R. *Chem. Rev.* **2005**, *105*, 2999−3094.
(56) Schmidt, M. W.; Baldridge, K. K.; Boatz, J. A.; Elbert, S. T.; Gordon, M. S.; Jensen, J. H.; Koseki, S.; Matsunaga, N.; Nguyen, K. A.; Su, S.; Windus, T. L.; Dupuis, M.; Montgomery, J. A. *J. Comput. Chem.* **1993**, *14*, 1347−1363.
(57) Gordon, M. S.; Schmidt, M. W. Chapter 41 - Advances in electronic structure theory: GAMESS a decade later. In *Theory and Applications of Computational Chemistry*; Dykstra, C. E., Frenking, G., Kim, K. S., Scuseria, G. E., Eds. Elsevier: Amsterdam, 2005; pp 1167−1189.
(58) Beveridge, D. L.; Schnuelle, G. W. *J. Phys. Chem.* **1975**, *79*, 2562−2566.
(59) Abraham, M. H.; Liszi, J.; Mészaros, L. *J. Chem. Phys.* **1979**, *70*, 2491−2496.
(60) Hoshi, H.; Sakurai, M.; Inoue, Y.; Chûjô, R. *J. Chem. Phys.* **1987**, *87*, 1107−1115.
(61) Bonaccorsi, R.; Scrocco, E.; Tomasi, J. *Int. J. Quantum Chem.* **1986**, *29*, 717−735.
(62) Cancès, E.; Mennucci, B.; Tomasi, J. *J. Chem. Phys.* **1997**, *107*, 3032−3041.
(63) Cancès, E.; Mennucci, B. *J. Math. Chem.* **1998**, *23*, 309−326.
(64) Pomelli, C. S.; Tomasi, J.; Barone, V. *Theor. Chem. Acc.* **2001**, *105*, 446−451.
(65) Li, H.; Pomelli, C. S.; Jensen, J. H. *Theor. Chem. Acc.* **2003**, *109*, 71−84.
(66) Cancès, E.; Mennucci, B. *J. Chem. Phys.* **2001**, *114*, 4744−4745.
(67) Cancès, E.; Mennucci, B. *J. Chem. Phys.* **2001**, *115*, 6130−6135.
(68) Chipman, D. M. *J. Chem. Phys.* **2000**, *112*, 5558−5565.
(69) Corni, S.; Tomasi, J. *J. Chem. Phys.* **2002**, *117*, 7266−7278.
(70) Pascual-Ahuir, J. L.; Silla, E.; Tomasi, J.; Bonaccorsi, R. *J. Comput. Chem.* **1987**, *8*, 778−787.
(71) Schmickler, W. *Chem. Phys. Lett.* **1995**, *237*, 152−160.
(72) Pecina, O.; Schmickler, W.; Spohr, E. *J. Electroanal. Chem.* **1995**, *394*, 29−34.
(73) Hartnig, C.; Koper, M. T. M. *J. Phys. Chem. B* **2004**, *108*, 3824−3827.
(74) Bard, A. J.; Faulkner, L. R. *Electrochemical Methods: Fundamentals and Applications*, 2nd ed.; Wiley: Hoboken, NJ, 2000.
(75) Grahame, D. C. *Chem. Rev.* **1947**, *41*, 441−501.
(76) Saveant, J.-M., *Elements of Molecular and Biomolecular Electrochemistry*. Wiley-Interscience: Hoboken, NJ, 2006.
(77) Gileadi, E. *J. Solid State Electrochem.* **2011**, *15*, 1359−1371.
(78) Frumkin, A. N. *Z. Phys. Chem.* **1933**, *164*, 121.
(79) Tsirlina, G. A.; Petrii, O. A.; Nazmutdinov, R. R.; Glukhov, D. V. *Russ. J. Electrochem.* **2002**, *38*, 132−140.
(80) Bockris, J. O. M.; Reddy, A. K. N.; Gamboa-Aldeco, M. E. *Modern Electrochemistry 2A: Fundamentals of Electrodics*, 2nd ed.; Springer: New York, 2001.

(81) Albery, W. J. *Electrode Kinetics*; Clarendon Press: Oxford, U.K., 1975.
(82) McLean, J. D.; Timnick, A. *Anal. Chem.* **1967**, *39*, 1669−1671.
(83) Gavaghan, D. J.; Feldberg, S. W. *J. Electroanal. Chem.* **2000**, *491*, 103−110.
(84) Baránski, A.; Fawcett, W. R. *J. Electroanal. Chem.* **1979**, *100*, 185−196.
(85) Kojima, H.; Bard, A. J. *J. Am. Chem. Soc.* **1975**, *97*, 6317−6324.
(86) Fawcett, W. R.; Lasia, A. *J. Phys. Chem.* **1978**, *82*, 1114−1121.
(87) Royea, W. J.; Krüger, O.; Lewis, N. S. *J. Electroanal. Chem.* **1997**, *438*, 191−197.
(88) Fawcett, W. R.; Kováčová, Z. *J. Electroanal. Chem.* **1990**, *292*, 9−32.
(89) Becke, A. D. *J. Chem. Phys.* **1993**, *98*, 5648−5652.
(90) Stephens, P. J.; Devlin, F. J.; Chabalowski, C. F.; Frisch, M. J. *J. Phys. Chem.* **1994**, *98*, 11623−11627.
(91) Hertwig, R. H.; Koch, W. *Chem. Phys. Lett.* **1997**, *268*, 345−351.
(92) *GAMESS manual*; Ames Laboratory, Iowa State University: Ames, IA, 2013; http://www.msg.chem.iastate.edu/gamess/documentation.html.
(93) Hehre, W. J.; Ditchfield, R.; Pople, J. A. *J. Chem. Phys.* **1972**, *56*, 2257−2261.
(94) Ditchfield, R.; Hehre, W. J.; Pople, J. A. *J. Chem. Phys.* **1971**, *54*, 724−728.
(95) Barone, V.; Cossi, M.; Tomasi, J. *J. Chem. Phys.* **1997**, *107*, 3210−3221.
(96) Gill, D. S. *Electrochim. Acta* **1979**, *24*, 701−703.
(97) Marcus, R. A. *J. Phys. Chem.* **1968**, *72*, 891−899.
(98) Costentin, C.; Louault, C.; Robert, M.; Roge, V.; Saveant, J.-M. *Phys. Chem. Chem. Phys.* **2012**, *14*, 1581−1584.
(99) Fawcett, W. R.; Fedurco, M. *J. Phys. Chem.* **1993**, *97*, 7075−7080.
(100) Rüssel, C.; Jaenicke, W. *J. Electroanal. Chem.* **1984**, *180*, 205−217.
(101) Ahlberg, E.; Parker, V. D. *Acta Chem. Scand.* **1983**, *37B*, 723−730.
(102) Winkler, K.; Baranski, A. S.; Fawcett, W. R. *J. Chem. Soc., Faraday Trans.* **1996**, *92*, 3899−3904.